INSTITUTE OF PHYSICS PUBLISHING PLASMA SOURCES SCIENCE AND TECHNOLOGY

Plasma Sources Sci. Technol. **15** (2006) 858–864 doi:10.1088/0963-0252/15/4/032

Time resolved measurements of the CF_2 rotational temperature in pulsed fluorocarbon rf plasmas

O Gabriel[1], **S Stepanov, M Pfafferott and J Meichsner**

Institute of Physics, University of Greifswald, Domstrasse 10a, D-17498, Greifswald, Germany

E-mail: meichsner@physik.uni-greifswald.de

Received 13 March 2006, in final form 2 August 2006
Published 10 October 2006
Online at stacks.iop.org/PSST/15/858

Abstract

Knowledge of the absolute densities of small radicals like CF, CF_2 and CF_3 in fluorocarbon plasmas is essential for a fundamental understanding of plasma chemical processes and plasma surface interaction. Infrared absorption spectroscopy by means of tunable diode lasers (IR-TDLAS) was established and widely used for density measurements in the last decade. The often unknown parameter in the calculation of absolute radical densities from a measured absorption of a single line is the rotational temperature. In particular, a strong dependence of the line strength on rotational temperature has a significant influence on density calculation. In this paper we report on measurements of the CF_2 rotational temperature in capacitively coupled CF_4/H_2 plasmas (CCP) with rf (13.56 MHz) powers up to 200 W. Rotational temperatures in continuous and pulsed modes of the discharge were found to be between 300 and 450 K. Furthermore, first measurements of the time dependence of the rotational temperature in pulsed rf plasma are presented. The rotational temperature rises in the plasma phase within 0.1 s and goes down again to the temperature of the background gas in the plasma pause within 0.5 s. It is also shown that accurate density measurements of the radicals by means of single line absorption need correct information about the rotational temperature and careful selection of a suitable absorption line.

1. Introduction

Low pressure plasma processing is a key technology in many branches of industry. For semiconductor microchip fabrication fluorocarbon radio frequency plasmas were successfully applied, e.g. for contact hole etching [1]. Furthermore, thin films deposited with this kind of plasma have a low dielectric constant making them interesting for insulating intermediate layers in order to reduce the layer capacitance and increase the performance of microchips [2, 3]. These amorphous fluorocarbon films are extremely cross-linked and highly chemical inert. Other useful properties are their repellence against water and oil [4] and their potential for biocompatibility [5]. Although these plasmas were studied for many years, details of the process mechanisms in the gas phase and at surfaces including transient molecular species are not well understood. It is known that the radicals CF, CF_2 and CF_3 are not only the main dissociation products of the feed gas (e.g. CF_4 or C_4F_8) but also play an important role in the etching and deposition process itself [6, 7]. The surfaces, e.g. substrates, electrodes and chamber walls are changed by the interaction of charged and neutral reactive plasma species, and the species densities in the gas phase are influenced by the surface processes and vice versa. Therefore, the measurement of the densities of radicals and stable molecules in the gas phase is essential for the understanding of these processes [8]. Various diagnostic methods like laser induced fluorescence spectroscopy [9–11], UV absorption spectroscopy [12–16] and ionization threshold mass spectrometry [17–19] were applied for this purpose. One method of obtaining absolute

[1] Present address: Department of Applied Physics, Eindhoven University of Technology, PO Box 513, 5600 MB Eindhoven, The Netherlands.

molecule densities is the infrared absorption spectroscopy, either done by means of broad band fourier transform infrared spectroscopy (FTIR) [20] or tunable diode laser absorption spectroscopy (TDLAS) [6, 21, 22]. These diagnostics do not disturb the plasma and they can provide other information such as molecule temperatures [23, 24].

In order to calculate an absolute species density from a measured absorption it is necessary to know the strength of the observed absorption line. This line strength depends on the rotational temperature T_{rot} due to the distribution of the species over the rotational levels within a vibrational band for a given temperature. The rotational temperature is often assumed to be close to room temperature as it was measured in previous works for capacitively coupled rf plasmas [20]. If absorption measurements are performed with lines that show only a slight dependence on T_{rot} the error in density calculation due to temperature variation may be neglected. But we will show that some absorption lines of CF_2 have a dependence on T_{rot} that is too strong to be neglected. Their line strengths vary with a factor of up to 2 for an increase in T_{rot} from room temperature up to 500 K. On the other hand this strong dependence of the used CF_2 absorption line on T_{rot} can be applied for temperature estimation by time resolved measurements of the absorption decay of just a single line in pulsed plasma. These temperatures will be compared with those that were gained by the conventional interpretation of a Boltzmann plot. Besides, first time resolved measurements of the CF_2 rotational temperature by means of a time-resolved Boltzmann plot in the pulsed plasma will be presented.

2. Experiment

The capacitively coupled rf plasma is produced in a cylindrical stainless steel chamber about 20 litres in volume (figure 1).

The powered electrode consists of a cylindrical copper block 8 cm in diameter that is placed in the centre of the chamber. A matching network couples the electrode capacitively to the 13.56 MHz rf power generator. The plasmas are maintained at rf powers up to 200 W in continuous or pulsed operation with pulse frequencies lower than 1 Hz. The chamber walls are grounded to produce a highly asymmetrical rf discharge. CF_4 and H_2 were used as process gases. The total pressure (10–100 Pa) and gas flow (1–10 sccm) are regulated independently by means of a capacitance manometer, mass flow controllers, a throttle valve controller and a sliding vane rotary pump. The process gases were fed through small holes at the top of the shielding of the rf electrode into the vacuum chamber.

The IR laser beam is guided in a double path through the chamber 4 cm above the rf electrode using KBr windows with a broad transparent range in the mid-IR. The total length of the double path through the plasma chamber amounts to 90 cm.

The IR radiation is produced by a tunable lead salt multimode diode laser. The operation temperatures of this kind of diode lasers are between 30 and 100 K. Therefore, a closed helium cycle is used to cool down the laser diodes. The emission frequency is set roughly by the operating temperature ($10\,\mathrm{cm^{-1}\,K^{-1}}$). Fine tuning of the frequency can be done very fast by modulating the diode current with a current ramp. Spectra can be measured with spectral resolutions of

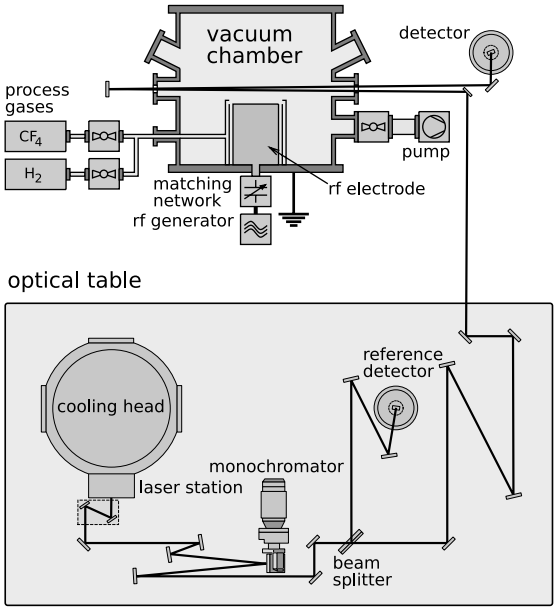

Figure 1. Experimental apparatus: vacuum chamber and TDLAS system.

$10^{-4}\,\mathrm{cm^{-1}}$ and time resolutions of 50 μs. A monochromator is used in order to select a desired laser mode. Various reference gas cells with well-known absorption lines, e.g. C_2H_4, N_2O, and a Germanium etalon in the reference beam path were applied to identify observed lines and measure their spectral positions correctly. However most of the radiation (about 90%) was available for the absorption measurements inside the reactor. The laser control and data acquisition software TDLWintel (Aerodyne Research, Inc., Billerica, USA) allowed recording of the measured data and doing a real-time spectra analysis. The calculation of molecule densities from measured absorption lines was performed assuming Voigt line profiles with the gas temperature, beam path length and line strengths as input parameters. Up to three different species, i.e. lines with three different absorption positions, can be analysed simultaneously in one spectral scan.

3. Spectra and line strengths of CF_2

The ratio between the measured intensity $I(\nu)$ due to the absorption in a medium (e.g. the gas phase of a plasma) and the initial intensity $I_0(\nu)$ without absorption is described in the case of linear spectroscopy by the well-known Lambert–Beer law

$$I(\nu)/I_0(\nu) = \mathrm{e}^{-k(\nu)L}, \tag{1}$$

where L is the absorption path length and $k(\nu)$ is the absorption coefficient depending on the wave number of the radiation. According to the notation by Penner [25], the line strength S is the proportional factor between the spectral integral over a single absorption line and the density n of the absorbing molecules

$$\int_{\mathrm{line}} k(\nu)\,\mathrm{d}\nu = S \cdot n. \tag{2}$$

In the case of ro-vibrational transitions within the same electronic ground state these rotational levels are mostly

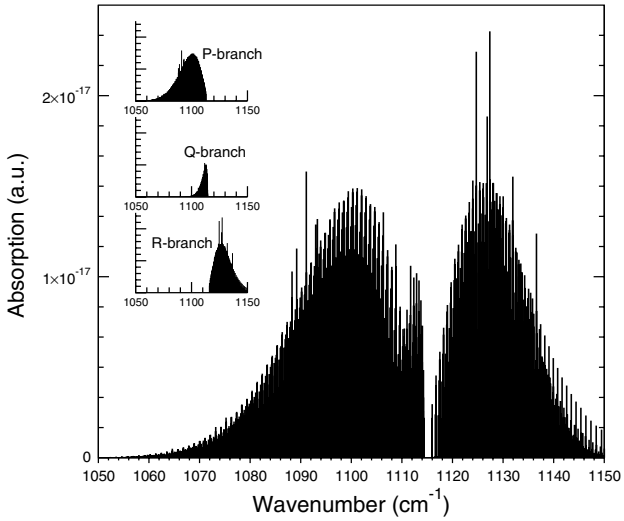

Figure 2. Calculated spectrum of the CF_2 ν_3 band. The insets show the P-, Q- and R-branch separately.

Boltzmann distributed, and then the line strength is given by

$$S = \frac{8\pi^3}{3hc}\nu_{12}\frac{g_1 A}{Q}\mu^2\,\mathrm{e}^{-E_1/(k_\mathrm{B}T)}, \tag{3}$$

where h—Planck constant, c—speed of light, ν_{12}—transition frequency, g_1—statistical weight of the lower level, A—Hönl-London factor, Q—partition function, E_1—energy of the lower level, k_B—Boltzmann constant, T—rotational temperature and μ—dipole moment of the transition. The dipole moment is a characteristic quantity of the vibration band of the molecule. For CF_2 it can be gained from absolute density measurements using UV absorption spectroscopy [14, 15].

The terms g_1, E_1, A and Q can be calculated with well-known formulae since CF_2 is very close to a symmetric rotator and its rotation constants are given in the literature [26, 27]. This was done for the absorption lines within the ν_3 band of CF_2. The resulting spectrum is shown in figure 2 and resembles very well the structure of the ν_3 band that was measured by Burkholder and Howard [27]. The single peaks in the band spectrum are due to overlapping of more than one absorption line, i.e. they lie closer to each other than the Doppler width of the lines ($\Delta\nu \approx 0.001\ \mathrm{cm}^{-1}$). The maxima of the P-, Q- and R-branch are centred at 1101, 1113 and 1126 cm^{-1}. The maxima of the P- and Q-branch were accessible with the available laser diodes in the presented experiment.

Equations (2) and (3) can be rearranged to a linear dependence between the energy E_1 and the logarithms of the weighted densities:

$$\ln\left(\frac{1}{g_1 A}\int_{\mathrm{line}} k(\nu)\,\mathrm{d}\nu\right) = -\frac{E_1}{k_\mathrm{B}T} + C, \tag{4}$$

where C is a constant. If the logarithms of the weighted densities (the left term of equation (4)) are plotted against the energies E_1, the result should be a straight line with the slope $-(k_\mathrm{B}T_\mathrm{rot})^{-1}$ (a Boltzmann-plot). This is only valid, if the rotational energy levels show a Boltzmann distribution. Therefore such a plot is also a suitable proof of the existence of this distribution.

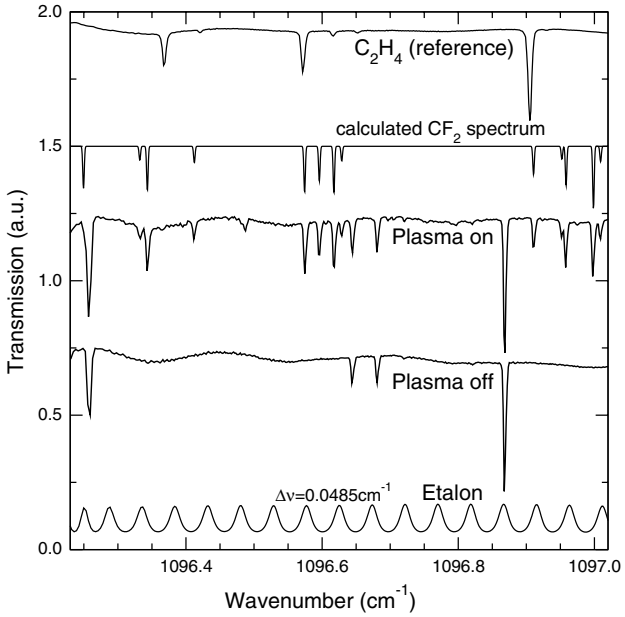

Figure 3. Absorption spectra measured during and after a CF_4/H_2 rf plasma compared with a C_2H_4 reference spectrum. The spectra contain several CF_2 lines (ν_3 P-branch) and four lines of a currently unknown stable product (see text). The etalon signal is also shown.

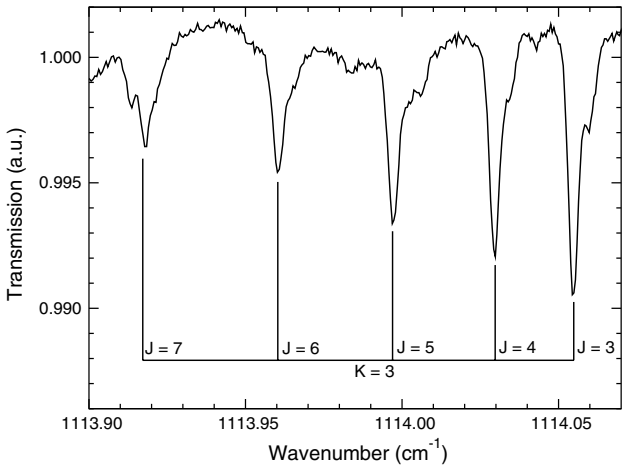

Figure 4. Measured part of the Q-branch of the CF_2 ν_3 band. The first five lines of the $K = 3$ series are shown.

In figure 3 various measured spectra in the range 1096–1097 cm^{-1} of the fundamental P-branch of CF_2 ν_3 band are shown. The calibration of absolute line positions was done by comparison with the well-known spectrum of C_2H_4 and an etalon signal. The exact positions of CF_2 absorption lines are listed in table 1. The spectrum contains 13 absorption lines of the CF_2 radical that are visible in the rf plasma but they vanish completely after switching off the discharge. However, four lines of a stable but currently unknown species still remain in the plasma off phase. These species are produced in the CF_4/H_2 plasma. Until now it was not possible to identify the species, but measurements with reference gases indicate that it is not CF_4, C_2F_6, C_3F_8, CH_4 or C_2H_4.

In figure 4 the first five measured absorption lines of the $K = 3$ series of the fundamental ν_3 Q branch of CF_2 are shown.

Table 1. Transitions and spectral positions of the measured CF_2 absorption lines [26].

Transition							Position
J''	K''_a	K''_c	→	J'	K'_a	K'_c	(cm^{-1})
P branch							
17	10	7		16	10	6	1096.4123
18	8	11		17	8	10	1096.9106
19	7	12		18	7	11	1096.5959
20	4	16		19	4	15	1096.9522
20	4	17		19	4	16	1096.9584
20	5	16		19	5	15	1096.6173
21	0	21		20	0	20	1096.9986
21	1	20		20	1	19	1096.5743
21	1	21		20	1	20	1097.0091
21	2	19		20	2	18	1096.3433
21	2	20		20	2	19	1096.6288
21	3	19		20	3	18	1096.3322
21	3	21		20	3	20	1096.2495
Q branch							
3	3	0		3	3	1	1114.0547
4	3	1		4	3	2	1114.0294
5	3	2		5	3	3	1113.9977
6	3	3		6	3	4	1113.9605
7	3	4		7	3	5	1113.9605

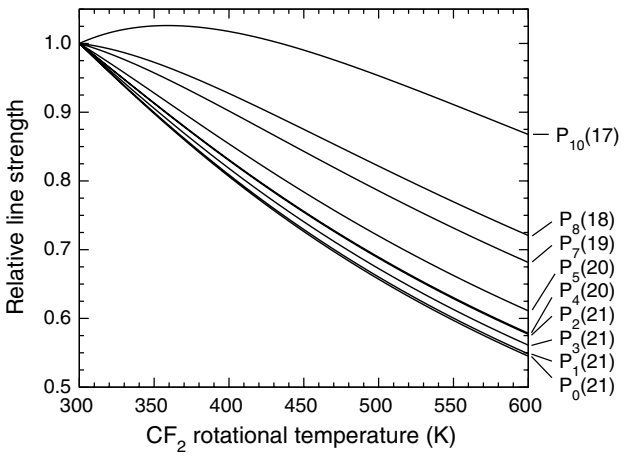

Figure 5. Calculated relative dependences of the line strengths on T_{rot} for several ν_3 P-branch lines of CF_2.

For all measured absorption lines, listed in table 1, the line strengths were calculated. Relative dependences of these line strengths on the rotational temperature are shown in figures 5 and 6. All five lines from the Q-branch show almost the same temperature dependence: a decay of a factor of 2 for an increase in T_{rot} from 300 to 500 K. These dependences on T_{rot} are so similar to each other, that it was impossible to determine the rotational temperature using a Boltzmann-plot.

In contrast to that, the strengths of the P-branch lines decrease in a more different way with increasing T_{rot}. The strength of the line $P_{10}(17)$ even increases slightly and has a maximum at 360 K. However, the strength of this line stays almost constant in the T_{rot} range between 300 and 500 K. Therefore, this line is the most suitable one within the P-branch for density measurements if the rotational temperature remains below 500 K.

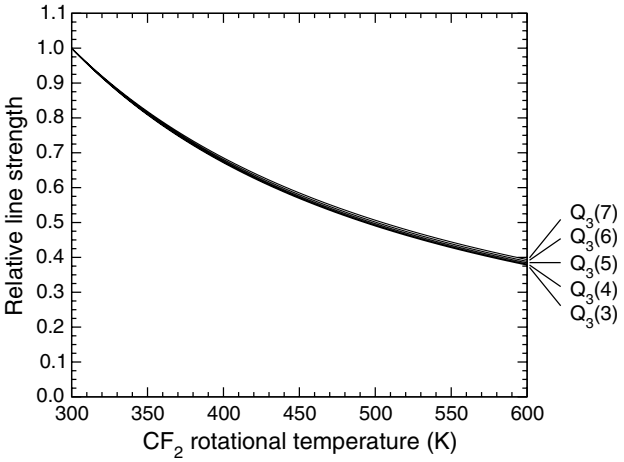

Figure 6. Calculated relative dependences of the line strengths on T_{rot} for the first five $K = 3$ lines of the ν_3 Q-branch lines of CF_2.

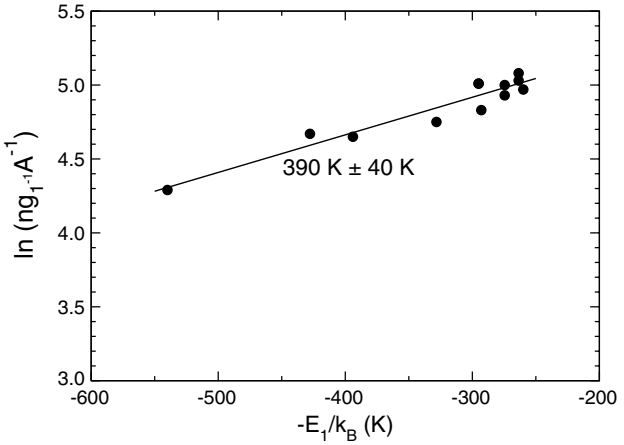

Figure 7. Boltzmann plot for 11 CF_2 absorption lines within the P-branch of ν_3-band (continuous plasma, 50 Pa, 5 sccm CF_4, 2 sccm H_2, 100 W).

4. CF_2 rotational temperatures in an rf plasma

4.1. CF_2 rotational temperature in continuous plasma

The measured absorption of 11 lines within the P branch of the CF_2 ν_3 band were used to perform a Boltzmann-plot. The result is shown in figure 7. The plotted logarithms of the weighted absorptions are sufficiently linear against the energy of the lower level E_1, i.e. the initial assumption of a Boltzmann distribution is valid. In the shown example the rotational temperature of CF_2 was calculated to be 390±40 K. This is a typical value for the rotational temperature of CF_2, which was also measured by others with broadband spectroscopic methods, i.e. 350 K in a 13.56 MHz rf plasma with FTIR [20] and 500±100 K in a 2/27 MHz rf plasma with UV absorption spectroscopy [16].

4.2. The time dependence of the CF_2 rotational temperature

It can be very important to take into account the time dependence of the line strength on the rotational temperature. This dependence and its influence on the CF_2 density determination was studied in pulsed rf plasmas at low pulse

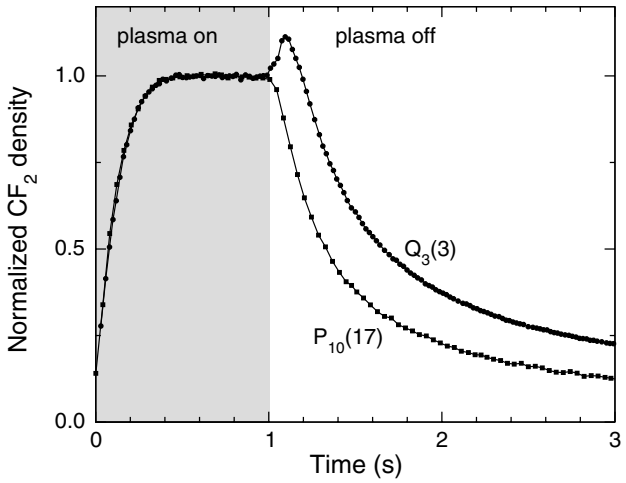

Figure 8. Development of the CF_2 density in a pulsed plasma (50 Pa, 5 sccm CF_4, 2 sccm H_2, 100 W) measured using two different absorption lines $Q_3(3)$ and $P_{10}(17)$.

frequencies. Figure 8 shows the development of the CF_2 density as it was measured by means of the absorption lines $Q_3(3)$ and $P_{10}(17)$. For better comparability the graphs are normalized to one at the end of the plasma on phase. The graph measured with the $P_{10}(17)$ line behaves as expected in the pulsed plasma: it rises in the plasma phase, reaches a constant density level and decays, more or less exponentially, back towards zero in the pulse pause. In contrast to this, the density measured with the $Q_3(3)$ line seems to abruptly increase directly after the discharge is off. Then it reaches a maximum value and decreases.

Such an initial increase of the CF_2 density in the afterglow was already measured by others [13, 28] and explained by the CF_2 production due to the chemical reactions of the neutral molecules [13] and/or by CF_2 fluxes due to changes in the gas temperature in the afterglow phase [28]. It is also clear that production mechanisms, in which electrons or ions take part, are not a likely reason for the CF_2 density increase, because the live times of charged plasma species in the afterglow are much lower in comparison with the observed CF_2 kinetics [29]. Moreover, the absorption was measured by using two different CF_2 lines under the same plasma conditions. Therefore, the observed difference of the normalized CF_2 concentrations is definitively caused by some features of the lines itself.

In our investigations the mentioned increase in CF_2 density finds a plausible explanation just by a change in its rotational temperature. We assume an exponential decay of T_{rot} from a higher value in the plasma $T_{rot,pl}$ down to the lower temperature $T_{rot,0}$ of the background gas. In the case of $P_{10}(17)$ line strength and for rotational temperatures lower than 500 K the CF_2 density determination is not significantly influenced by rotational temperature changes. Therefore, the normalized CF_2 density profile for the $P_{10}(17)$ absorption line in figure 8 represents the true density behaviour.

In contrast to this the density calculation using a $Q_3(3)$ line is strongly determined by the rotational temperature. When T_{rot} decreases after the plasma on phase from the value in plasma $T_{rot,pl}$ back to the temperature of the background gas $T_{rot,0}$ (approximately room temperature), the $Q_3(3)$ line strength will increase. Since the line strength is a fixed input

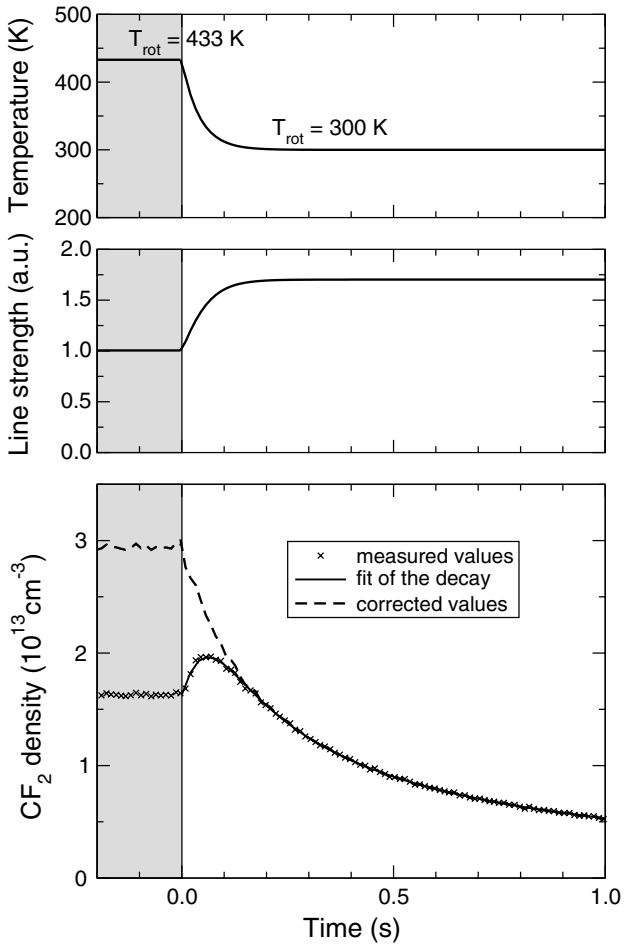

Figure 9. Assumed development of T_{rot} and its influence on $Q_3(3)$ line strength and the measured CF_2 density.

parameter in the calculation procedure used by the TDLWintel software, the result of this calculation is an increasing density (according to equation (2)). This effect together with the real decay in CF_2 density in the plasma off phase forms the observed maximum of the density (see figure 8).

The assumed time dependence of T_{rot} in the afterglow, the resulting variation of $Q_3(3)$ line strength, and its influence on the measured CF_2 densities are shown in figure 9. By a decrease in T_{rot} the line strength increases and therefore the measured density, too. This is the result of the real-time calculation of the density based on the absorption at a constant rotational temperature. Following this, the temperature $T_{rot,pl}$ and the time constant of its decay in the off phase were used as parameters to describe the measured CF_2 densities in the afterglow. The resulting fit is also shown in figure 9. It describes the measured values very well. Finally, the measured values can be corrected. One can see that the CF_2 density in the plasma phase is almost twice higher than the measured one. This is due to almost twice the lower strength of the $Q_3(3)$ line at $T_{rot} = 430$ K compared with the value at room temperature.

Since $T_{rot,pl}$ was used as a parameter to describe the CF_2 decay curves it is also possible to gain $T_{rot,pl}$ by the measurement of the absorption decays of just a single line. This is in contrast to a Boltzmann-plot, where several absorption lines have to be measured simultaneously. It should also be

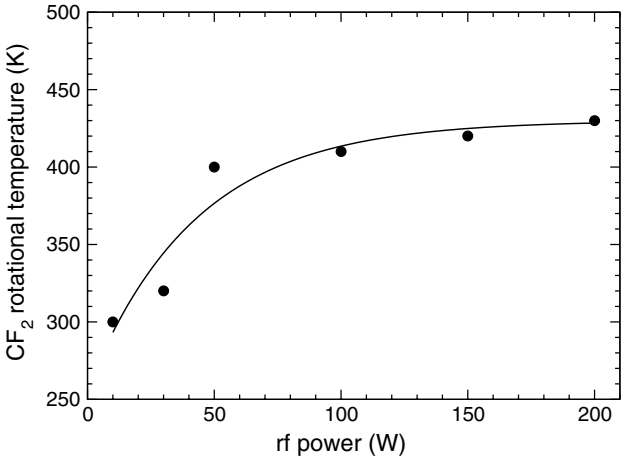

Figure 10. The dependence of estimated $T_{rot,pl}$ on the rf power (50 Pa, 8 sccm CF_4, 2 sccm H_2, $t_{on} = 5$ s, $t_{off} = 5$ s).

noted that this method is only practicable in the case of a sufficiently long living species like CF_2. The life time has to be longer than the decay time of the rotational temperature.

As shown in figure 10 the method was successfully applied to estimate the rotational temperature of CF_2 in the plasma. In this figure $T_{rot,pl}$ is shown for several rf powers. The main error in this estimation is due to the absorption method (TDLAS) by means of the integrated values over the line of sight, i.e. over the total beam path way through the reactor. The density measurements as well as the results of the rotational temperatures are not spatially resolved; therefore, they represent only mean values over the total path length. So, the increase in $T_{rot,pl}$ in figure 10 may also be influenced by an extension of the active plasma zone. At rf powers of 50–100 W the active zone reaches its maximum volume and also the temperature reaches a constant value and does not increase further with rising rf power. This is more in agreement with measurements of Littau *et al* , who did not find any dependence of $T_{rot,pl}$ on the rf power in an ICP, but an almost constant value of about 360 K [24]. The explanation is that the higher rf powers mean higher electron densities in the plasma, but the electron energy distribution stays nearly constant, resulting in a constant rotational temperature for CF_2.

Additionally, the experimental set-up allowed us to measure the absorption of up to three lines simultaneously. In particular, it was possible to measure the absorption of three neighbouring CF_2 lines, $P_3(21)$, $P_2(21)$ and $P_{10}(17)$, with a high time resolution of 10 ms. Their line strengths have a very different dependence on the rotational temperature (see figure 5), that allowed us to perform a Boltzmann-plot for each of the measured triads. The result is the time dependence of the CF_2 rotational temperature for the investigated pulsed plasma, see figure 11.

As one can see, the rotational temperature reaches a constant value in the plasma on phase very fast, within 100 ms. The following decay back to the temperature of the background gas (just above 300 K) in the pulse pause is distinctly slower, with a time constant of about 0.5 s. The strong scattering of the measured T_{rot} at the end of the plasma off phase is due to the decreasing measured absorption (decreasing CF_2 density). This measured T_{rot} time profile also proves our initial

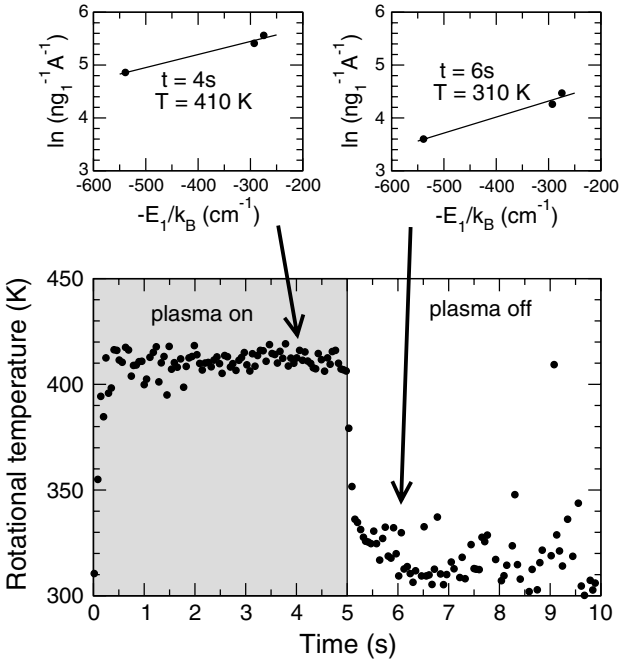

Figure 11. The time dependence of T_{rot} in a pulsed plasma. In addition two Boltzmann-plots for the data points at 4 and 6 s are shown on top (50 Pa, 8 sccm CF_4, 2 sccm H_2, 100 W).

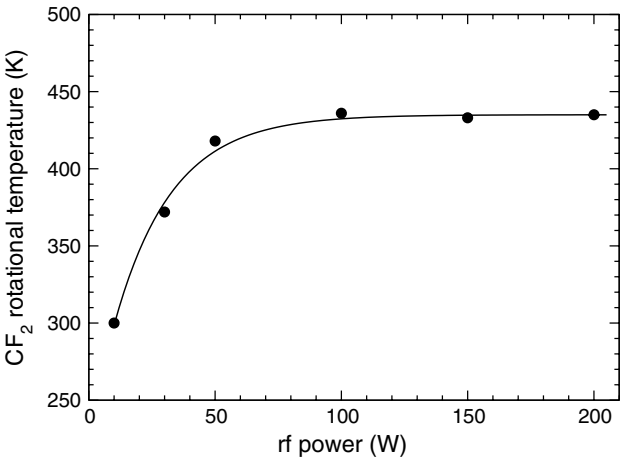

Figure 12. The dependence of $T_{rot,pl}$ gained from a Boltzmann-plot on the rf power (50 Pa, 5 sccm CF_4, 2 sccm H_2, $t_{on} = 1$ s, $t_{off} = 2$ s).

assumption of the exponential decay which was made above for the estimation of $T_{rot,pl}$ from a single absorption line, (see figure 9). Finally, the values of $T_{rot,pl}$ measured by means of the time resolved Boltzmann-plots in dependence on the rf power are shown in figure 12. The result is similar to the one presented in figure 10. The difference between them is obviously caused by slightly different plasma conditions.

5. Conclusions

For correct relative and absolute density measurements by means of absorption spectroscopy in the mid-IR, knowledge of the rotational temperature T_{rot} is essential. For the CF_2 radicals we showed that the densities calculated from a measured absorption can vary with a factor of about 2 if the rotational

temperature changes from room temperature to $T_{rot} = 500$ K. Therefore, the assumption of rotational temperature being close to room temperature may cause significant errors, especially in a pulsed rf plasma with low pulse frequencies, where T_{rot} changes quickly between room temperature and a steady-state value in the plasma phase. Here the time dependence of the rotational temperature should be known. We also measured T_{rot} using different methods involving spectral parts in the P- and Q-branch of the fundamental ν_3 band of CF_2. The time resolved measurements show that T_{rot} in the plasma phase reaches a steady-state value about 400–500 K very fast, within 100 ms. In the pulse pause it decays back to the background gas temperature distinctly slower, with time constants of about 0.5 s. With the knowledge of this time dependence of T_{rot} the measured densities can be easily corrected.

Acknowledgments

This work was supported by the Federal Ministry of Education and Research in Germany (BMBF) under Grant No 13N8051 and by the Deutsche Forschungsgemeinschaft (DFG) in the frame of the SFB-TRR24, Project B5.

References

[1] Tachi S 2003 *J. Vac. Sci. Technol.* A **21** S131
[2] Capps N E, Mackie N M and Fisher E R 1998 *J. Appl. Phys.* **84** 4736
[3] Theil J A 1999 *J. Vac. Sci. Technol.* B **17** 2397
[4] Chase J E and Boerio F J 2003 *J. Vac. Sci. Technol.* A **21** 607
[5] Limb S J, Gleason K K, Edell D J and Gleason E F 1997 *J. Vac. Sci. Technol.* A **15** 1814
[6] Goto T and Hori M 1996 *Japan. J. Appl. Phys.* **35** 6521
[7] Inayoshi M, Ito M, Hori M, Goto T and Hiramatsu M 1998 *J. Vac. Sci. Technol.* A **16** 233
[8] Hori M and Goto T 2006 *Plasma Sources Sci. Technol.* **15** S74
[9] Hargis P J and Kushner M J 1982 *Appl. Phys. Lett.* **40** 779
[10] Booth J-P, Hancock G, Perry N D and Toogood M J 1989 *J. Appl. Phys.* **66** 5251
[11] Fendel P, Francis A and Czarnetzki U 2005 *Plasma Sources Sci. Technol.* **14** 1
[12] d'Agostino R, Cramarossa F, Colaprica V and d'Ettole R 1983 *J. Appl. Phys.* **54** 1284
[13] Cruden B A, Gleason K K and Sawin H H 2001 *J. Appl. Phys.* **89** 915
[14] Wormhoudt J and McCurdy K E 1989 *Chem. Phys. Lett.* **158** 480
[15] Suto O and Steinfeld J 1990 *Chem. Phys. Lett.* **168** 181
[16] Bulcourt N, Booth J-P, Hudson E A, Luque J, Mok D K W, Lee E P, Chau F-T and Dyke J M 2004 *J. Chem. Phys.* **120** 9499
[17] Hikosaka Y, Toyoda H and Sugai H 1993 *Japan. J. Appl. Phys.* **32** L353
[18] Stoffels E, Stoffels W W and Tachibana K 1998 *Rev. Sci. Instrum.* **69** 116
[19] Geigl M, Peters S, Gabriel O, Krames B and Meichsner J 2005 *Contrib. Plasma Phys.* **45** 369
[20] Haverlag M, Stoffels W W, Stoffels E, den Boer J H W G, Kroesen G M W and de Hoog F J 1995 *Plasma Sources Sci. Technol.* **4** 260
[21] Schaepkens M, Martini I, Sanjuan E A, Li X, Oehrlein G S, Perry W L and Anderson H M 2001 *J. Vac. Sci. Technol.* A **19** 2946
[22] Nakamura M, Hori M, Goto T, Ito M and Ishii N 2001 *J. Appl. Phys.* **90** 580
[23] Haverlag M, de Hoog F-J and Kroesen G M W 1991 *J. Vac. Sci. Technol.* A **9** 327
[24] Littau M E, Sowa M J and Cecchi J L 2002 *J. Vac. Sci. Technol.* A **20** 1603
[25] Penner S S 1959 *Quantitative Molecular Spectroscopy and Gas Emissivities* (Reading, MA: Addision-Wesly)
[26] Davies P B, Hamilton P A, Elliot J M and Rice M J 1983 *J. Mol. Spectrosc.* **102** 193
[27] Burkholder J B and Howard C J 1988 *J. Mol. Spectrosc.* **127** 362
[28] Booth J-P, Abada H, Chabert P and Graves D B 1998 *Plasma Sources Sci. Technol.* **14** 273
[29] Kono A, Haverlag M, Kroesen G M W and de Hoog F-J 1991 *J. Appl. Phys.* **70** 2939